

# Robust Interest Point Detection by Local Zernike Moments

Gökhan Özbulak and Muhittin Gökmen

*Department of Computer Engineering, Istanbul Technical University, Istanbul, Turkey*

**Keywords:** Interest Point Detection, Feature Extraction, Object Detection, Local Zernike Moments, Scale-Space.

**Abstract:** In this paper, a novel interest point detector based on Local Zernike Moments is presented. Proposed detector, which is named as Robust Local Zernike Moment based Features (R-LZMF), is invariant to scale, rotation and translation changes in images and this makes it robust when detecting interesting points across the images that are taken from same scene under varying view conditions such as zoom in/out or rotation. As our experiments on the Inria Dataset indicate, R-LZMF outperforms widely used detectors such as SIFT and SURF in terms of repeatability that is main criterion for evaluating detector performance.

## 1 INTRODUCTION

In computer vision, general object detection framework is based on i) extracting interesting points in images, ii) describing regions around these points as feature vectors and iii) matching feature vectors in order to find corresponding points of the images. For instance, if there are two images of one scene containing a black car, by detecting interesting points that qualify the car itself in both images and searching for similarity between feature vectors extracted around these points through some distance metrics such as Euclidean or Mahalanobis, it's possible to say that the black car in first image exists in the second image as well. This point correspondence is also important for stereo vision, motion estimation, image registration and stitching applications to be able to match corresponding regions in images.

Searching for corresponding points between images is a hard problem when these images are scaled, rotated and/or translated versions of each other. Under these geometric transformations, interesting points still need to be detected and matched with high repeatability score that is the correspondence rate of the interesting points detected between the images.

A good interest point detector is expected to be invariant to geometric and photometric transformations, and also robust to background clutters and occlusions in image. Changes in scale, rotation and translation between the images are examples of geometric transformations whereas

illumination change is an example of photometric transformations. Scale invariance problem is handled by building scaled samples of the image with Gaussian blurring and then applying the interest point detector to these samples. This stack of images is named as scale-space and it's widely used by well-known methods such as Scale Invariant Feature Transform (SIFT) (Lowe, 2004) and Speeded-Up Robust Features (SURF) (Bay et al., 2008). Local characteristics of interest points make them invariant to background clutters and occlusions (Mikolajczyk and Schmid, 2004). The locality also provides translational invariance for interest point detectors because local regions move together in the image and thus information in a local region is preserved in case of image translation.

In this paper, by extending our previous rotation-invariant detector named as Local Zernike Moment based Features (LZMF) (Özbulak and Gökmen, 2014), we propose a robust interest point detector that is invariant under scale, rotational and translational changes. Proposed method uses rotation-invariant Zernike moments locally in the bility scores for "Zoom&Rotationn order to detect interesting points and thus exhibits rotation and translation-invariant characteristics. For scale invariance, a scale-space is constructed from given image and interest point detector is applied to images in spatial and scale-space in order to detect interest points/keypoints. We name our interest point detector as Robust Local Zernike Moment based Features or R-LZMF shortly.

## 2 RELATED WORK

In the literature, most of interest point detection schemas are based on corner or blob detectors because they are good candidates to be interesting points. One of the earliest interest point detector was developed by Harris et al. and named as Harris corner detector (Harris and Stephens, 1988). It searches for large intensity changes in spatial-space by sliding a window and detects such locations as corners. Harris detector is rotation-invariant but not scale-invariant.

Andrew Witkin introduced the scale-space theory in his seminal work (Witkin, 1983) and showed that convolving an image with Gaussian filters of increasing sigma repeatedly exposes the structures in different scales and thus gives scale invariance characteristic to the detector building it. Lindeberg extended the work of Witkin and proposed automatic scale selection mechanism with scale normalized Laplacian-of-Gaussian (LoG) operator to detect blob-like structures in an image (Lindeberg, 1998). Lowe, in (Lowe, 2004), showed that LoG can be approximated by Difference-of-Gaussian (DoG) that is the difference of two images convolved with Gaussian filters of consecutive sigma values. Lowe built DoG space for interest point detection and he presented a complete schema (detector and descriptor) named as Scale Invariant Feature Transform (SIFT).

Mikolajczyk et al. proposed Harris-Laplace detector, which combines Harris detector with LoG operator, in (Mikolajczyk and Schmid, 2001). They used Harris detector to localize interest points in 2D (spatial-space) and LoG operator to find local maximum in 3D (scale-space). The reason of using Laplacian instead of Harris function in 3D is that Harris function can't reach to maximum in scale-space frequently and this causes a few numbers of keypoints to be generated. Harris-Laplace detector was then extended in (Mikolajczyk and Schmid, 2002, 2004) by determining the shape of the elliptical region with the second moment matrix. This schema was named as Harris-Affine detector. Hessian-Affine detector, which detects interest points based on the Hessian matrix in 2D space, was also proposed in (Mikolajczyk and Schmid, 2002, 2004). Both Harris-Affine and Hessian-Affine detectors have significant invariance to affine transformations when compared with Harris-Laplace detector.

Bay et al., in their schema named as Speeded-Up Robust Features (SURF) (Bay et al., 2008), used Hessian-based detector instead of Harris-based

counterpart because Hessian function is more stable and repeatable. They preferred building scale-space of approximated LoG filters rather than image itself as opposed to SIFT and Harris-Laplace. Up-scaling the filters instead of down-scaling the image prevents aliasing problems occurred when sub-sampling the image and this approach is also faster than SIFT because up-scaled filters are implemented with efficient integral image method.

Rosten et al. developed a fast interest point detector and named it as Features from Accelerated Segment Test (FAST) in (Rosten and Drummond, 2006). FAST tests each image pixel for cornerness by looking its 16 pixel-circular neighborhood and if some contiguous pixels in this neighborhood are brighter/darker than the pixel in test then it's detected as corner. This method also learns from image pixels by applying decision tree to increase its accuracy. Interest points detected by FAST are not multi-scale features, in other words, FAST is not scale-invariant. Oriented FAST and Rotated Brief (ORB), proposed in (Rublee et al., 2011), is a combination of FAST keypoint detector and BRIEF descriptor (Calonder et al., 2010). ORB modifies FAST to work with image pyramid for scale invariance and it also modifies BRIEF descriptor to make it rotation-invariant. Center Surround Extrema (CenSurE) is another scale and rotation-invariant interest point detector proposed in (Agrawal et al., 2008). In CenSurE, a center-surround filter is applied to the image at all locations and scales, and Harris function is used for eliminating weak corner points. Leutenegger et al. proposed a rotation and scale-invariant key point detector named as Binary Robust Invariant Scalable Keypoints (BRISK) in (Leutenegger et al., 2011). BRISK uses a novel scale-space FAST-based detector for scale-invariant interest point detection and considers a saliency criterion by using quadratic function fitting in continuous domain.

In (Özbulak and Gökmen, 2014), we proposed a rotation-invariant interest point detector by applying Zernike moment of  $A_{42}$  to the image locally in order to measure cornerness and sweeping up nearby edges by dividing Zernike moments  $A_{42}$  to  $A_{40}$ . We named it as Local Zernike Moment based Features (LZMF). Performance evaluation of LZMF with "Rotation" sequence of the Inria Dataset showed that our method outperforms well-known interest point detectors such as SIFT, SURF, CenSurE and BRISK. In this study, we extend our rotation-invariant detector to be scale-invariant by building scale-space with optimal parameter settings.

### 3 ROBUST INTEREST POINT DETECTION

In this section, we introduce our robust and local Zernike Moment (LZM) based interest point detector schema, R-LZMF. Zernike moments are described in Section 3.1 and Section 3.2 includes a general overview of the proposed detector. In Section 3.3, we show how the scale-space is built in order to yield the best scale-invariance performance with our detector.

#### 3.1 Zernike Moments

In (Zernike, 1934), Fritz Zernike introduced a complete set of complex polynomials, named as Zernike polynomials, that are orthogonal on the unit disk  $x^2 + y^2 \leq 1$ . Zernike polynomials are defined as:

$$V_{nm}(x, y) = V_{nm}(\rho, \theta) = R_{nm}(\rho)e^{jm\theta} \quad (1)$$

Where  $R_{nm}(\rho)$  is the radial polynomial,  $n$  is the order of polynomial,  $m$  is the number of iteration,  $\rho$  is the length of vector from origin to  $(x, y)$  and  $\theta$  is the angle between  $\rho$  and x-axis in counter-clockwise direction. There are some constraints on  $n$  and  $m$  parameters such as  $n \geq 0$ ,  $n - |m| = \text{even}$  and  $|m| \leq n$ .  $R_{nm}(\rho)$  is defined as:

$$R_{nm}(\rho) = \sum_{s=0}^{\frac{n-|m|}{2}} \frac{(-1)^s \rho^{n-2s} (n-s)!}{s! \left(\frac{n+|m|}{2}-s\right)! \left(\frac{n-|m|}{2}-s\right)!} \quad (2)$$

Teague introduced using Zernike polynomials as orthogonal image moments in (Teague, 1980) for two-dimensional pattern recognition. Given an image function of  $f(x, y)$ , Zernike moment of order  $n$  and repetition  $m$  is defined as:

$$A_{nm} = \frac{n+1}{\pi} \iint_{x^2+y^2 \leq 1} f(x, y) V_{nm}^*(\rho, \theta) dx dy \quad (3)$$

Where  $*$  in  $V_{nm}^*(\rho, \theta)$  denotes the complex conjugate. The formula in (3) is discretized in order to work with digital images of size  $M \times N$  as:

$$A_{nm} = \frac{n+1}{\pi} \sum_{i=0}^{M-1} \sum_{j=0}^{N-1} f(i, j) V_{nm}^*(\rho_{ij}, \theta_{ij}) \Delta x_i \Delta y_j \quad (4)$$

Where  $x_i, y_j \in [-1, 1]$ ,  $\rho_{ij} = \sqrt{x_i^2 + y_j^2}$ ,

$\theta_{ij} = \tan^{-1} y_j/x_i$  and  $\Delta x_i = \Delta y_j = 2/N\sqrt{2}$ .

As seen from (4), a Zernike moment,  $A_{nm}$ , is a measurement about the intensity profile of the whole image. It's also possible to project the local intensity

profiles on to Zernike polynomials by fitting the unit circle on the pixels of the image. The image moments using Zernike moments in this way are named as local Zernike moments or LZM shortly. LZM presents a powerful description of local image region as it's successfully applied to face recognition problem in (Sariyanidi et al., 2012) and used for detection of low-level features such as step edges and gray-level corners in (Ghosal and Mehrotra, 1997). In this paper, we use LZM representation to detect gray-level corners by convolving the image with LZM based operator,  $V_{nm}^k$ .  $V_{nm}^k$  is a  $k \times k$  convolutional filter for Zernike moment of order  $n$  and repetition  $m$  and defined as:

$$V_{nm}^k(i, j) = V_{nm}(\rho_{ij}, \theta_{ij}) \quad (5)$$

An image is convolved with  $V_{nm}^k$  as below:

$$A_{nm}^k(i, j) = \sum_{p, q = -\frac{k-1}{2}}^{\frac{k-1}{2}} f(i-p, j-q) V_{nm}^k(p, q) \quad (6)$$

There is one real filter denoted as  $Re[V_{nm}^k]$  and one imaginary filter denoted as  $Im[V_{nm}^k]$  for a Zernike moment of order  $n$  and repetition  $m$  because Zernike moments are complex. However, imaginary filter is discarded when there is no repetition ( $m = 0$ ) and the image is only convolved with real filter.

The magnitude of Zernike moments is unchanged when an image is rotated by an angle of  $\alpha$  w.r.t. x-axis. This property gives Zernike moments rotation-invariant characteristic under image rotations, see (Khotanzad and Hong, 1990). The magnitude of Zernike moment is defined as:

$$|A_{nm}| = \sqrt{(Re[A_{nm}])^2 + (Im[A_{nm}])^2} \quad (7)$$

Where  $Re[A_{nm}]$  and  $Im[A_{nm}]$  are local Zernike moment representations obtained by convolving an image with real and imaginary Zernike filters,  $Re[V_{nm}^k]$  and  $Im[V_{nm}^k]$ , respectively. As a note,  $Im[A_{nm}]$  is zero and discarded when  $m = 0$ .

#### 3.2 Interest Point Detection by LZM

Our interest point detection method is applied in spatial (2D) and scale-space (3D). In spatial-space, input image is first converted to gray-scale and then  $L_2$ -normalization is applied on the gray-scaled image to make proposed detector more robust to noise as we showed in (Özbulak and Gökmen, 2014).

Before convolving the image with Zernike filter, a second normalization procedure is locally applied to the region where unit circle is fitted. The local intensity profile under this circle is fitted to standard

normal distribution with  $\mu = 0$  and  $\sigma = 1$  in order to make proposed detector more robust to local illumination changes. This is similar to normalization procedure in Normalized Cross-Correlation (NCC) and feature vector normalization in SIFT (Lowe, 2004).

The input image is then convolved with Zernike filters,  $V_{42}^9$  and  $V_{40}^9$ . Ghosal, in (Ghosal and Mehrotra, 1997), used Zernike filters with order of 2,  $V_{22}$  and  $V_{20}$ , for his corner detection schema. In the experiments, however, we found that working with more complex orders such as 4 yields better results in terms of repeatability. In our method, the magnitude of Zernike moment of  $A_{42}$ ,  $|A_{42}|$ , is used to measure the cornerness. A pre-defined corner threshold is applied to  $|A_{42}|$  response and the pixels that are higher than this threshold are considered as candidate interest points. The drawback of using Zernike moment of  $A_{42}$  is that it may respond to edges closer to corners. We suppress these nearby edges by dividing  $|A_{42}|$  to  $|A_{40}|$  as  $\frac{|A_{42}|}{|A_{40}|}$  and then thresholding  $\frac{|A_{42}|}{|A_{40}|}$  with a pre-defined nearby edge threshold. Candidate interest points passing this thresholding test are retained for further processing and the rest is discarded. So, in this way, interest points/keypoints, which are corners but not nearby edges, are considered. For proposed detector, corner threshold value of 0.51 and nearby-edge threshold value of 5, which were determined in our previous work by using "Rotation" sequence of the Inria Dataset, are used throughout the experiments.

A further refinement procedure by Non Maximum Suppression is also applied to the detected interest points in spatial domain as follows: i) a 5x5 window is centered on each interest point, ii) the interest point is compared based on  $|A_{42}|$  with detected interest points in its 5x5 neighborhood, iii) the interest point is retained if its  $|A_{42}|$  response is the maximum or discarded otherwise. In this way, redundant interest points are swept out and more consistent interest points are retained.

Candidate interest points detected in spatial-space are then examined in scale-space to eliminate weak ones, which don't reach local maximum in scale-space, and to figure out characteristic scales of strong ones (see Section 3.3 for details). This analysis is realized in each octave of the scale-space as follows: For outermost scale levels of an octave, candidate interest points detected as a result of spatial analysis are directly retained without any scale analysis. For inner scale levels of an octave, a candidate interest point is compared with interest points detected in lower and upper scale levels based

on  $|A_{42}|$ . This comparison again falls in 5x5 neighborhood of the point in interest for adjacent scale levels. If  $|A_{42}|$  response of the interest point is the maximum among all interest points detected in lower and upper scale levels then the candidate interest point is considered as a real interest point. This kind of approach is also named as 3D Non Maximum Suppression. Here, R-LZMF has  $5 \times 5 \times 3 = 75 - 1 = 74$  comparisons at most in spatial and scale-space and this check doesn't take time because it only compares the point in interest with detected interest points in 2D and 3D space, and stops comparison if one interest point in the neighborhood has higher  $|A_{42}|$ .

### 3.3 Scale-Space

Andrew Witkin introduced the scale-space concept in his seminal work (Witkin, 1983) to represent signals in different scale levels in order to show how signal behaviour changes from fine to coarse scales. He also showed that smoothing an image with Gaussian filters of increasing sigma has ability to suppress fine details and expose coarse structures. Koenderink, in (Koenderink, 1984), showed that Gaussian filter is the unique filter for building scale-space. Lindeberg verified this uniqueness and proposed an automatic scale selection mechanism in order to find the characteristic scale of an interesting point in an image (Lindeberg, 1998). Characteristic scale is the scale level where an interest point detection function reaches local extremum in the scale-space. This is the moment an image point exhibits most interesting characteristic (cornerness, blobness etc.) in the scale-space. A description extracted from an interest point with characteristic scale size would be independent of same interest points detected in different scaled images.

In this study, we build a scale-space for our rotation-invariant interest point detector proposed in our previous work to make it scale-invariant as well. The input image is repeatedly convolved with Gaussian filters of increasing sigma size for blurring and each blurred image constitutes a scale level,  $L(x, y, \sigma)$ , in the scale-space.  $L(x, y, \sigma)$  is defined as:

$$L(x, y, \sigma) = G(x, y, \sigma) * I(x, y) \quad (8)$$

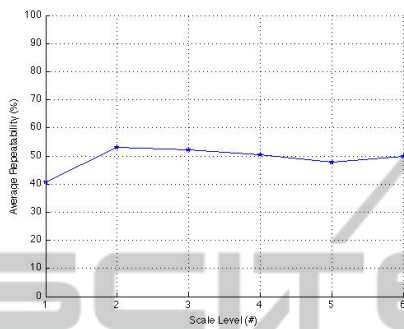
Where  $I(x, y)$  is the input image and  $G(x, y, \sigma)$  is the 2D Gaussian function defined as:

$$G(x, y, \sigma) = \frac{1}{2\pi\sigma^2} e^{-(x^2+y^2)/2\sigma^2} \quad (9)$$

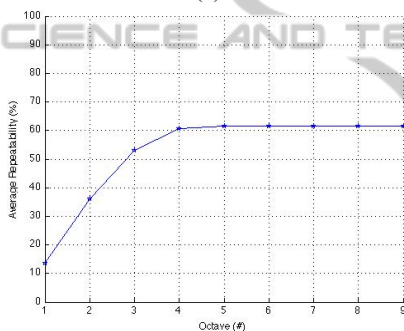
We divide scale-space into octaves for efficient computation. An octave is a stack of scale



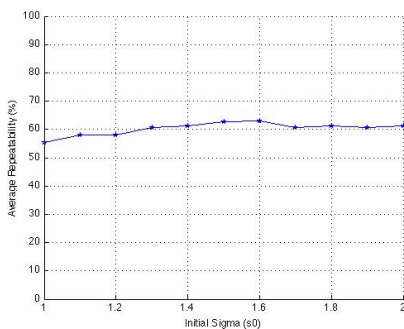
levels/layers,  $L(x, y, \sigma)$ , with same resolution and sigma for each scale level is a constant factor of previous scale layer's sigma. An image in one octave is a sub-sampled version of an image in previous octave. When sigma in an octave is doubled, the image convolved with Gaussian filter of this sigma is halved in size and used as first scale layer of next octave. Here, sub-sampling is the key factor for computational gain.



(a)



(b)



(c)

Figure 1: Parameter evaluation for scale-space based on average repeatability: (a) Number of scale level performance for  $o = 3$ ,  $s_0 = 1.7$ . (b) Number of octave performance for  $l = 2$ ,  $s_0 = 1.7$ . (c) Initial sigma performance for  $o = 4$ ,  $l = 2$ .

There are some parameters that should be fine-tuned in order to have a full coverage of scale-space. These are the number of scale levels in one octave ( $l$ ), the number of octaves in scale-space ( $o$ ) and

initial sigma for first scale level of the first octave ( $s_0$ ). We used Belledonnes images from “Zoom” sequence of the Inria Dataset to figure out the optimum parameters for our detector. We first determined the number of scale layer under assumptions of  $o = 3$  and  $s_0 = 1.7$  and got the best average repeatability by using two scale levels ( $l = 2$ ), see Figure 1-a. In this case, however, 3D Non Maximum Suppression is not applied because outermost scale layers are the only scale layers to be used. We then searched for the optimum number of octaves with  $l = 2$  under assumption of  $s_0 = 1.7$  and as seen from Figure 1-b working with 4 octaves ( $o = 4$ ) yields the best result in terms of average repeatability. As noted, using more than 4 octaves doesn't affect the performance. For initial sigma value, under  $o = 4$  and  $l = 2$ , although the best repeatability performance is obtained with value of 1.6 as seen in Figure 1-c, we had better performance with value of 1.8 ( $s_0 = 1.8$ ) in the experiments, so we use this value as initial sigma value. Thus, final parameter settings were determined as  $o = 4$ ,  $l = 2$  and  $s_0 = 1.8$ .

In Figure 2, the interest points detected by R-LZMF can be seen as red circles in some Laptop images of “Zoom&Rotation” sequence. In this figure, most of the interesting points detected in one image can be observed in other images as an indicator of how our detector is accurate in terms of repeatability.

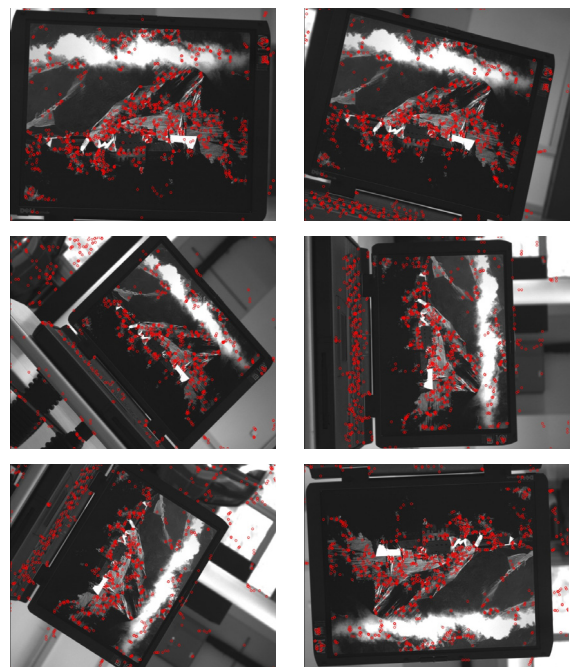


Figure 2: Interest points detected by R-LZMF for some Laptop images from “Zoom&Rotation” sequence.

### 4 EXPERIMENTAL RESULTS

The Inria Dataset is used for performance evaluation of proposed detector. We used Asterix, Crolles, VanGogh image sets from "Zoom" sequences, and East\_park, Laptop, Resid image sets from "Zoom&Rotation" sequences. "Zoom" sequence contains only scaled image sets and "Zoom&Rotation" image sets have scaled and rotated images. Image sets in both sequences have their own transformation matrices for repeatability evaluation although scale and rotation information about image sets are not provided. Therefore, x-axis in Figure 3 and Figure 4 show the image index instead of scale value or rotation angle. One can think of larger image index as larger scale and rotation angle.

As proposed in (Schmid et al., 1998), the repeatability score is main criterion to evaluate performance of interest point detectors. The repeatability is a measurement of the point correspondence between two images that are transformed form (scaled, rotated or translated) of each other. A robust interest point detector is expected to detect the most of the same structures in two images even they are scaled, rotated or translated versions of each other. The repeatability score is evaluated as:

$$r_{1,2} = \frac{C(f_1, f_2)}{\min(m_1, m_2)} \tag{10}$$

Where  $C(f_1, f_2)$  is the number of corresponding points detected in both images,  $m_1$  and  $m_2$  are the numbers of the keypoints detected in first and second images respectively.

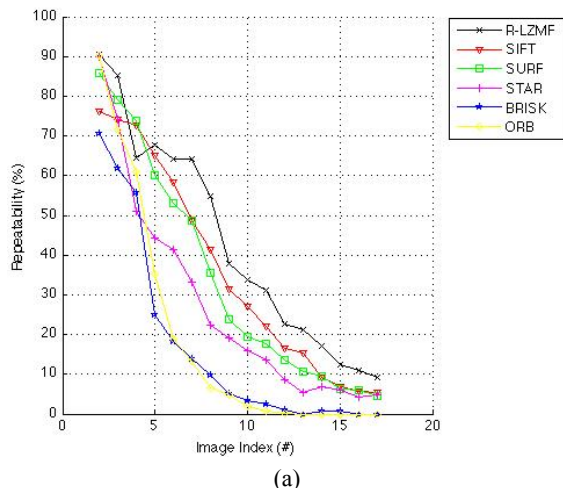
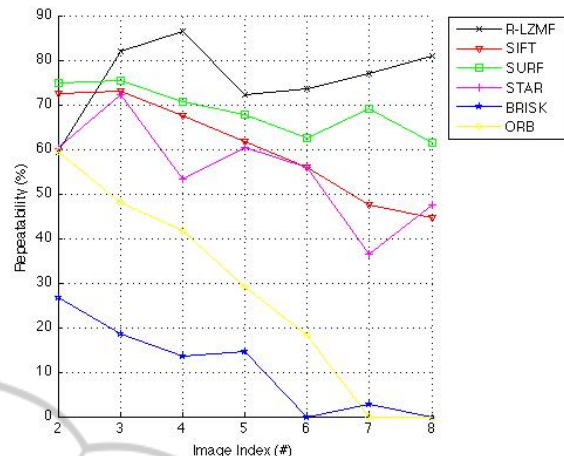
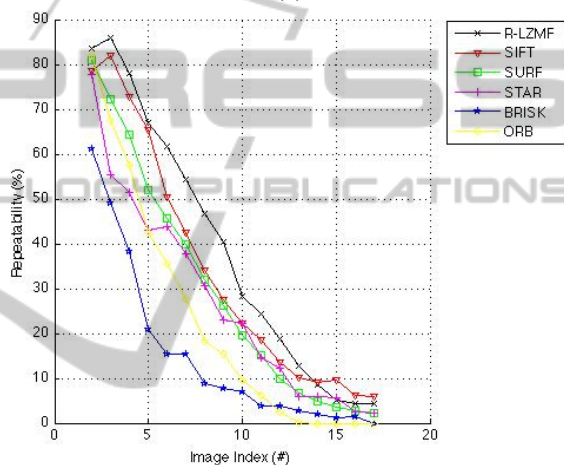


Figure 3: Repeatability scores for "Zoom" sequence: (a) Asterix. (b) Crolles. (c) VanGogh.



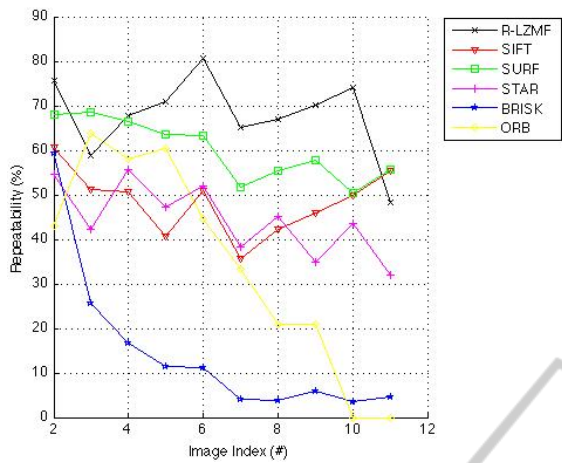
(b)



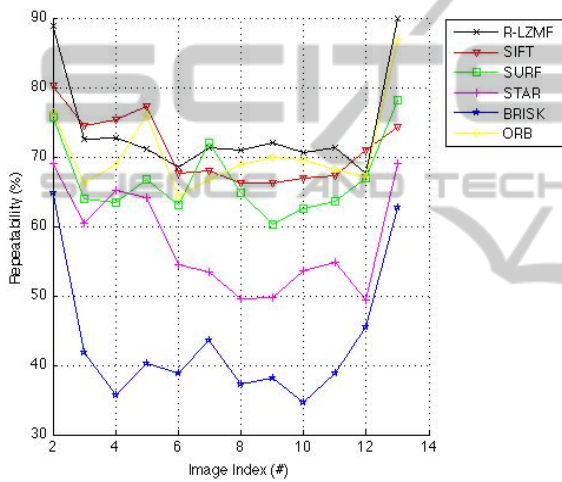
(c)

Figure 3: Repeatability scores for "Zoom" sequence: (a) Asterix. (b) Crolles. (c) VanGogh (cont.).

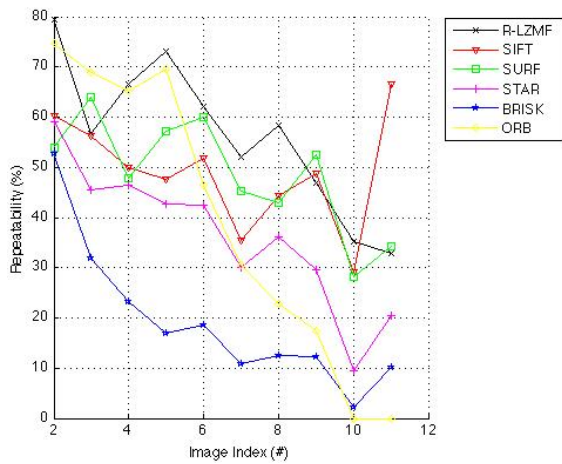
Repeatability performance of R-LZMF with image sets used for evaluation is plotted in Figure 3 for "Zoom" sequence and in Figure 4 for "Zoom&Rotation" sequence. As seen from plots, R-LZMF outperforms well-known detectors such as SIFT, SURF, CenSurE (STAR), BRISK and ORB for all image sets. We used OpenCV v2.4.8 to work with these detectors and applied them on the image sets with default parameter settings. As a note, throughout the experiments, we used our detector with same parameter settings as well: corner threshold=0.51, nearby-edge threshold=5,  $\sigma = 4$ ,  $l = 2$ ,  $s_0 = 1.8$ . From the bar charts in Figure 5, it can be seen that R-LZMF has also the best performance in terms of average repeatability when compared with all other detectors.



(a)

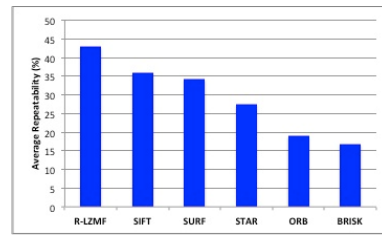


(b)

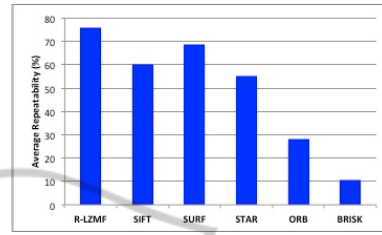


(c)

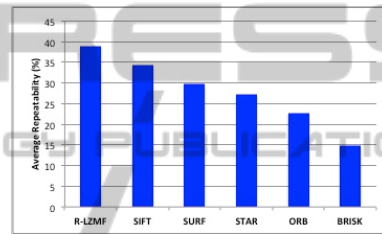
Figure 4: Repeatability scores for “Zoom&Rotation” sequence: (a) East\_park. (b) Laptop. (c) Resid.



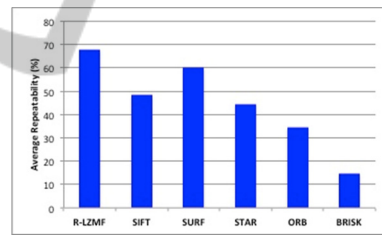
(a)



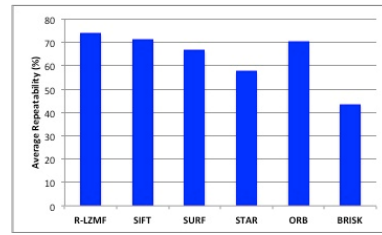
(b)



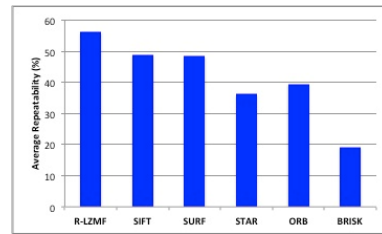
(c)



(d)



(e)



(f)

Figure 5: Average repeatability scores for: (a) Asterix. (b) Crolles. (c) VanGogh. (d) East\_park. (e) Laptop. (f) Resid.



## 5 CONCLUSIONS

In this paper, we proposed a novel interest point detector named as Robust Local Zernike Moment based Features or R-LZMF. This detector is based on local Zernike moments and invariant to geometric transformations such as scale, rotation and translation. We validated its robustness to these transformations by testing it with the Inria Dataset and reported that R-LZMF outperforms SIFT, SURF, CenSurE (STAR), BRISK and ORB for all image sets in the experiments. As a future work, we plan to analyse the performance of R-LZMF for affine transformation as well. Furthermore, we will extend R-LZMF to have a descriptor by using LZM again to utilize from its descriptive power so that it will be a complete schema (detector and descriptor) as in SIFT and SURF.

## REFERENCES

- Agrawal, M., Konolige, K., Blas, M. R., 2008. CenSurE: Center surround extremas for realtime feature detection and matching. *In European Conference on Computer Vision*, pp. 102-115.
- Bay, H., Ess, A., Tuytelaars, T., Gool, L.V., 2008. SURF: Speeded Up Robust Features. *In Computer Vision and Image Understanding*, vol. 110, no. 3, pp. 346-359.
- Calonder, M., Lepetit V., Strecha, C., Fua, P., 2010. BRIEF: Binary Robust Independent Elementary Features. *In European Conference on Computer Vision*, pp. 778-792.
- Ghosal, S., Mehrotra, R., 1997. A moment based unified approach to image feature detection. *In IEEE Trans. Image Processing*, vol. 6, no. 6, pp. 781-793.
- Harris, C., Stephens, M., 1988. A combined corner and edge detector. *Alvey Vision Conference*, pp. 147-151.
- Khotanzad, A., Hong, Y. H., 1990. Invariant image recognition by Zernike moments. *In IEEE Trans. Pattern Analysis and Machine Intelligence*, vol. 12, pp. 489-497.
- Koenderink, J.J., 1984. The structure of images. *Biological Cybernetics*, 50:363-396.
- Leutenegger, S., Chli, M., Siegwart R., 2011. BRISK: Binary Robust Invariant Scalable Keypoints. *In International Conference on Computer Vision*, pp. 2548-2555.
- Lindeberg, T., 1998. Feature detection with automatic scale selection. *In International Journal of Computer Vision*, 30(2):79-116.
- Lowe, D.G., 2004. Distinctive image features from scale-invariant keypoints. *In International Journal of Computer Vision*, vol. 60, no. 2, pp. 91-110.
- Mikolajczyk, K., Schmid, C., 2001. Indexing based on scale invariant interest points. *In International Conference on Computer Vision*, pp. 525-531.
- Mikolajczyk, K., Schmid, C., 2002. An affine invariant interest point detector. *In European Conference on Computer Vision*, pp. 128-142.
- Mikolajczyk, K., Schmid, C., 2004. Scale and affine invariant interest point detectors. *In International Journal of Computer Vision*, vol. 60, no. 1, pp. 63-86.
- Özbulak, G., Gökmen, M., 2014. A rotation invariant local Zernike moment based interest point detector. *In Proc. SPIE of International Conference on Machine Vision*.
- Rosten, E., Drummond, T., 2006. Machine learning for high-speed corner detection. *In European Conference on Computer Vision*, pp. 430-443.
- Rublee, E., Rabaud, V., Konolige, K., Bradski, G., 2011. ORB: an efficient alternative to SIFT or SURF. *In International Conference on Computer Vision*, pp. 2564-2571.
- Sariyanidi, E., Dagli, V., Tek, S.C., Tunc, B., Gokmen, M., 2012. Local Zernike Moments: A new representation for face recognition. *In International Conference on Image Processing*, pp. 585-588.
- Schmid, C., Mohr, R., Bauckhage, C., 1998. Comparing and evaluating interest points. *In IEEE International Conference on Computer Vision*, pp. 230-235.
- Teague, M.R., 1980. Image analysis via the general theory of moments, *In J. Optical Soc. Am.*, Vol. 70, pp. 920-930.
- The Inria Dataset, <http://lear.inrialpes.fr/people/mikolajczyk/Database>.
- Witkin, A.P., 1983. Scale-space filtering. *In International Joint Conference on Artificial Intelligence*, Karlsruhe, Germany, pp. 1019-1022.
- Zernike, F., 1934. *Physica*, vol. 1.